JCTC Journal of Chemical Theory and Computation

Article

pubs.acs.org/JCTC

Excitons in Organics Using Time-Dependent Density Functional Theory: PPV, Pentacene, and Picene

S. Sharma,*[,†,‡] J. K. Dewhurst,[†] S. Shallcross,[¶] G. K. Madjarova,[†,§] and E. K. U. Gross[†]

[†]Max-Planck-Institut für Mikrostrukturphysik, Weinberg 2, D-06120 Halle, Germany

[‡]Department of Physics, Indian Institute of Technology, Roorkee, 247667 Uttarkhand, India

[¶]Lehrstuhl für Theoretische Festkorperphysik, Staudstr. 7-B2, 91058 Erlangen, Germany

[§]Department of Physical Chemistry, Faculty of Chemistry and Pharmacy, Sofia University, 1126 Sofia, Bulgaria

ABSTRACT: We apply the bootstrap kernel within time-dependent density functional theory to study the one-dimensional chain of polymer polyphenylenevinylene and molecular crystals of picene and pentacene. The absorption spectra of poly(p-phenylenevinylene) has a bound excitonic peak that is well-reproduced. Pentacene and picene, electronically similar materials, have remarkably different excitonic physics, and this difference is also well captured. We show that the inclusion of local-field effects dramatically changes the spectra of both picene and pentacene but not for poly(*p*-phenylenevinylene).

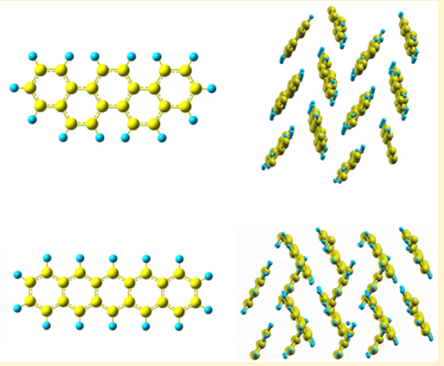

1. INTRODUCTION

Given the current urgency of investing in renewable energy sources, it is difficult to overstate the importance of energy efficient optoelectronic materials such as organic solar cells. The crucial information required in the controlled design of these systems is the optical absorption edge and spectra of the material, especially in the low-energy region close to the band edge. This is, in turn, dominated by the physics of bound electron−hole pairs known as excitons. Currently, the most prominent and state-of-the-art method to calculate an accurate absorption spectra in the presence of excitons is to solve the Bethe-Salpeter equation (BSE),[1,2] a computationally expensive scheme that becomes even more cumbersome for the systems of interest in solar-cell technology, which typically have a few 100 atoms per unit cell. Time-dependent density functional theory (TDDFT)[3] is an alternative route to calculate the exact absorption spectra with orders of magnitude less computational effort. However, the accuracy of the TDDFT approach rests entirely on the approximation employed for the exchange-correlation (xc) kernel, and the design of such a functional to correctly describe the excitonic physics has posed a perennial challenge to the TDDFT community.[4−7]

In this regard, the recently proposed bootstrap kernel[8] has shown very promising results for the absorption spectra of periodic solids.[8,9] The bootstrap kernel was designed d on three-dimensional, cubic, inorganic solids (II−IV and III−V insulators), and it is not clear that the same bootstrap procedure will work for low-dimensional or highly anisotropic, organic systems which constitute the materials of interest for modern optoelectronic devices. In view of this, we apply the TDDFT with bootstrap approximation to a set of organic materials; the one-dimension chain of poly(p-phenylenevinylene) (PPV) and the molecular crystals of picene and pentacene.

The choice of this set of materials is motivated by the fact that each member is well-known to possess a rich excitonic physics[10−12] that cannot be captured by simple xc kernels such as the random-phase approximation (RPA) or adiabatic local density approximation (ALDA),[13] and as such, they present an ideal test bed for the bootstrap kernel.

PPV, an example of an optoelectronic material [a one-dimensional (1D) chain of PPV has been used in the production of energy-efficient light-emitting diodes], for which excitonic effects play a crucial role.[14−17] A one-dimensional chain of PPV exhibits a bound excitonic peak below the fundamental gap,[14] and this system is therefore an ideal candidate for testing the accuracy of any new xc kernel for 1D organic polymers.

Picene and pentacene are extended solids with the constituent molecular units bound by the van der Waals force. This weak binding results in crystals in which the electronic properties are mainly determined by the individual molecular units, which provide yet another test case for the applicability of the bootstrap kernel. Despite possessing very similar structures and single particle spectra, picene and pentacene exhibit strikingly different excitonic physics. In the former, excitons are primarily of the Frenkel type[18,19] while the

Received: February 10, 2015

DOI: 10.1021/acs.jctc.5b00133
J. Chem. Theory Comput. XXXX, XXX, XXX−XXX

latter has a large charge transfer character to the exciton.[12,20,21] In addition, one finds that pentacene displays a strong Davydov splitting of the spectra, while picene does not.[21−23] These pronounced spectral differences between two structurally and electronically very similar materials presents a further severe test for any xc kernel. With these tests, we hope to show that TDDFT calculations with bootstrap approximation to the xc kernel are computationally efficient and have reliable accuracy and hence can easily be used to screen 1000s of organic crystals in search for better optoelectronic devices.

2. METHODOLOGY

2.1. Formalism. The TDDFT equation for the dielectric function is given by (atomic units are used):

$$\varepsilon^{-1}(\mathbf{q}, \omega) = 1 + v(\mathbf{q})\chi(\mathbf{q}, \omega)$$
$$= 1 + \chi_0(\mathbf{q}, \omega)v(\mathbf{q}) \times [1 - (v(\mathbf{q}) + f_{xc}(\mathbf{q}, \omega))\chi_0(\mathbf{q}, \omega)]^{-1} \quad (1)$$

where $f_{xc}(\mathbf{q},\omega)$ is the xc kernel, v is the bare Coulomb potential, χ is the fully interacting response function, and χ_0 is the response function of the noninteracting Kohn−Sham system. The construction of an efficient scheme for the optical spectra within TDDFT necessitates a heuristic partition of the xc kernel in eq 1 as a sum of two terms, $f_{xc} = f_{xc}^{(1)} + f_{xc}^{(2)}$. While this partition of the xc kernel is not unique, it delineates two distinct aspects of the optical response: (1) the physics of the single particle spectrum and (2) the excitonic physics. Single particle band gaps calculated using local or semilocal approximations to the xc potential within DFT are well-known to be underestimated. In order to obtain the correct band structure, one must, for example, perform a computationally expensive GW calculation. However, precisely the same physics can be obtained by the xc kernel without recourse to many-body perturbation theory; $f_{xc}^{(1)}$ is such a kernel and is responsible for correcting the underestimated band gap. The second part of the xc kernel, $f_{xc}^{(2)}$, is responsible for capturing the excitonic physics. The Dyson equation, eq 1, may then be written as

$$\varepsilon^{-1}(\mathbf{q}, \omega) = 1 + \chi_{gc}(\mathbf{q}, \omega)v(\mathbf{q}) \times [1 - (v(\mathbf{q}) + f_{xc}^{(2)}(\mathbf{q}, \omega))\chi_{gc}(\mathbf{q}, \omega)]^{-1} \quad (2)$$

where

$$\chi_{gc}(\mathbf{q}, \omega) = [1 - \chi_0(\mathbf{q}, \omega)f_{xc}^{(1)}(\mathbf{q}, \omega)]^{-1}\chi_0(\mathbf{q}, \omega) \quad (3)$$

is the gap corrected Kohn−Sham response function of the system. For all further calculations, we simply replace χ_{gc} by the response function calculated from the scissor operator-corrected Kohn−Sham band structure − unoccupied Kohn−Sham eigenvalues are rigidly shifted to higher energies to make the Kohn−Sham and exact fundamental band gap equal. In order to keep the whole procedure parameter free, the value of the fundamental band gap can be calculated using the GW method.[10,12,24] The RPA is equivalent to setting $f_{xc}^{(2)} = 0$, and the bootstrap kernel[8] consists of approximating $f_{xc}^{(2)}$ by

$$f_{xc}^{boot}(\mathbf{q}, \omega) = \varepsilon^{-1}(\mathbf{q}, \omega = 0)[\chi_0(\mathbf{q}, \omega = 0)]^{-1} \quad (4)$$

where ε_0 is the RPA dielectric tensor. In the bootstrap approach, eqs 4 and 2 are solved self-consistently. All the quantities (in eqs 1, 2, 3, and 4) are matrices in the basis of reciprocal lattice vectors **G** and have the following structure:

$$\begin{bmatrix} \varepsilon_{xx} & \varepsilon_{xy} & \varepsilon_{xz} & \text{wings} \\ \varepsilon_{yx} & \varepsilon_{yy} & \varepsilon_{yz} & 3 \times (n_{\mathbf{G}} - 1) \\ \varepsilon_{zx} & \varepsilon_{zy} & \varepsilon_{zz} & \\ \text{wings} & & & \text{body} \\ (n_{\mathbf{G}} - 1) \times 3 & & & (n_{\mathbf{G}} - 1) \times (n_{\mathbf{G}} - 1) \end{bmatrix}$$

where $n_{\mathbf{G}}$ is the number of **G** vectors. Such a matrix needs to be inverted to solve eq 1. In the original work on the bootstrap kernel[8] and earlier works with the nanoquanta kernel[5] and long-range kernel,[4,6] eq 1 is separately solved for each component. In such a case, the head is just a single c-number and the wings have dimension $(n_G - 1)$. This procedure is fully justified for a cubic system; however, for noncubic systems, such a procedure is a severe approximation,[25] and all the components of the dielectric tensor must be calculated together by using such a full matrix for χ_0.

Due to the nature of the bootstrap kernel (see numerator of eq 4), f_{xc} also inherits this structure from ε^{-1} and transforms like a tensor (which is also an exact property of the kernel). As for the denominator, in the original work[8] only the head of ε_0 was used and without any loss of generality the same can be done here too. However, keeping in mind the highly anisotropic nature of the materials studied in the present work, we propose not just the head but also the body of the RPA dielectric function, ε_0, be used (the wings of ε_0 in eq 4 are set to 0). We note that for cubic materials, studied in the original work, this does not have any effect on the results.

2.2. Efficiency of the Method. All calculations have been performed using the full-potential linearized augmented plane wave method[26] as implemented in the Elk code.[27] To achieve convergence for PPV, we required 16 × 1 × 1 **k**-point mesh, 60 empty states (19 occupied states), and 51 **G**-vectors. A smearing width of 0.12 eV was used for calculating the optical spectra. In the case of pentacene and picene, convergence required 8 × 6 × 3 **k**-point mesh, 40 empty states (102 occupied states), and 87 **G**-vectors. Optical spectra were calculated using a smearing width 0.08 eV. The calculated G_0W_0 gaps were found to be 4.09 eV for picene and 2.08 eV for pentacene.

The most expensive part of the bootstrap calculation is constructing the matrix χ_0. If one were to consider only the heads of the matrices in eqs 1−4, the method becomes exceptionally computationally efficient. Choosing head-only approximation is equivalent to ignoring local field effects (LFE). In Figure 1 is shown the time needed for calculation of

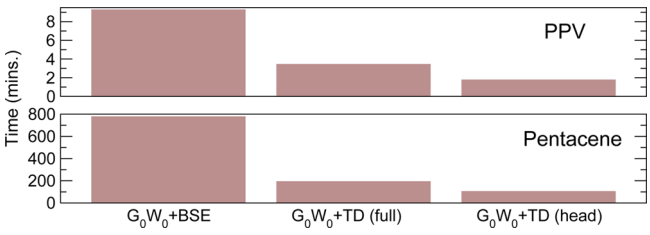

Figure 1. Time (in mins) required for BSE and TDDFT calculations for PPV (top) and pentacene (bottom). All calculations are performed in parallel on 8 processors.

DOI: 10.1021/acs.jctc.5b00133
J. Chem. Theory Comput. XXXX, XXX, XXX−XXX

spectra for PPV and pentacene. Three facts are clear from this figure: (1) G_0W_0+TDDFT calculation is far more computationally efficient as compared to G_0W_0+BSE; (2) the head-only bootstrap method is more efficient than the full bootstrap method; (3) assuming that the bootstrap method has an accuracy comparable to BSE for organic insulators, and we will show that is the case for the materials considered here, then the computational bottleneck shifts from the calculation of optical properties to the calculation of the electronic ground state. As there exist very efficient schemes for calculating the ground state, for instance the Tran-Blaha functional[28,29] which gives correct band gap (but not necessarily the band-structure) eliminating the need to perform G_0W_0 calculations, it is clear that TDDFT can form the basis for the high-throughput screening of organic insulators for a desired optical property.

3. RESULTS

For very large systems, the head only version of bootstrap is much quicker than a full bootstrap calculation, and thus, we first check the quality of TDDFT calculations using only the heads of the matrices in eqs 1−4. The quality check is performed by comparing the results with full BSE calculations and/or experimental data.

3.1. 1D PPV Chain. Isolated PPV chain displayed in Figure 2 is a conjugated polymer with 8 carbon atoms and 6 hydrogen

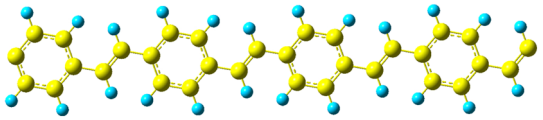

Figure 2. 1D poly(p-phenylenevinylene) chain.

atoms per unit cell.[10] The results for the imaginary part of the dielectric function, ε_2, for PPV obtained with the electric field polarized along the direction of the chain are presented in the top panel of Figure 3. The physics of the bound electron−hole

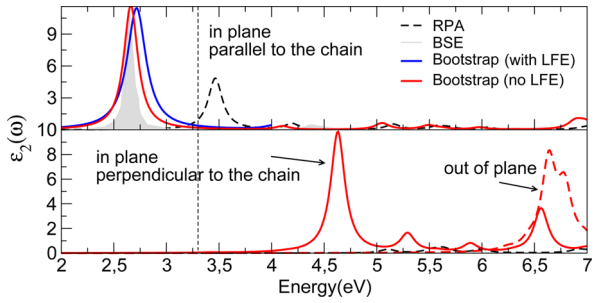

Figure 3. Dielectric tensor for PPV obtained using the bootstrap kernel, RPA, and by solving BSE as a function of energy (in electronvolts). The quasi-particle gap is indicated by a dashed (black) line.

pair is, as expected, totally missing in the RPA results which show a peak just above the quasi-particle gap at 3.3 eV (shown as black dotted line in Figure 3). On the other hand, the results obtained using the bootstrap kernel show a strongly bound excitonic peak at 2.66 eV. These results are in good agreement with the experimental absorption data[14] which shows the first transition peak at 2.5 eV. It is well-known experimentally[16] that for ordered polymers, the strength of the peak at 2.5 eV is much larger than the peak at 6 eV, as seen in the present work. It is also clear from Figure 3 that the TDDFT results are in excellent agreement with the dielectric function obtained by solving the BSE. It is important to point that the BSE results obtained in the present work (shown as (gray) shaded area in Figure 3) are in excellent agreement with previous calculations.[10,24] Other than the main peak at 2.5 eV, the experimental absorption data[14,16] shows transitions at 3.7, 4.8, and 6 eV. All these transitions are also well-reproduced by the bootstrap kernel that shows peaks at 4.04, 5.05, and 5.8−6 eV. Solving the full TDDFT problem, which is equivalent to the inclusion of LFE, does not change the spectrum significantly.

The lower panel of Figure 3 shows the dielectric function obtained using different electric field configurations: the electric field in the plane of the polymer but perpendicular to the chain and the electric field perpendicular to the polymer plane. In both cases, the RPA spectrum is very different from the TDDFT spectrum, with the later always showing a large excitonic peak.

3.2. Molecular Crystals. We now turn our attention towards the organic molecular crystals. Linear acenes like picene and pentacene have attracted much attention[30−32] due to the presence of large charge-carrier mobilities needed for field-effect transistors. For these systems at the level of single molecule calculation, Grimme and Parac[33] demonstrated that applying TDDFT with traditional and global hybrid functionals fail in correctly describing low-lying excited states. More sophisticated long-range-corrected density functionals[34] or double-hybrids[35] were also applied to investigate the exciton energies, and it was demonstrated[21] that the large charge transfer character of excitons in pentacene plays a major role in the photo physics of the single crystals and can be used as a direct pathway to singlet fission,[36] converting high-energy photons into multiple electron−hole pairs, making the study of low-energy excitons in these crystals of particular importance.

Both picene and pentacene are polycyclic aromatic hydrocarbons composed of five benzene rings that for pentacene are made up of linearly fused benzene rings joined in zigzag conformation,[37,38] while for picene are in the armchair conformation[39] (for details see Figure 4).

As a first step, we calculate the ground-state and, as expected, find that the Kohn−Sham gaps obtained using LDA within DFT are small (2.45 eV for picene and 0.68 eV for pentacene) and a scissors correction is needed to make the Kohn−Sham

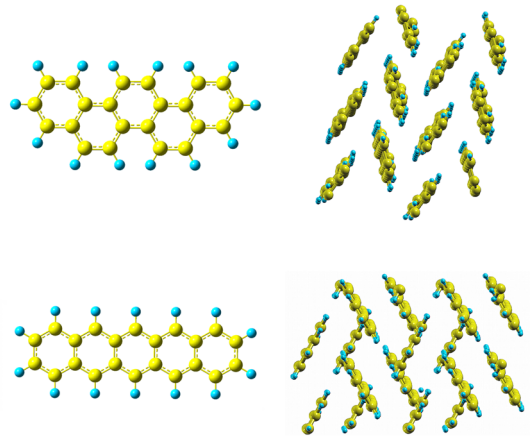

Figure 4. Molecular and crystalline structure of picene (top) and pentacene (bottom).

DOI: 10.1021/acs.jctc.5b00133
J. Chem. Theory Comput. XXXX, XXX, XXX−XXX

gap equal to the quasi-particle gap,[12,20] which is 4.08 eV for picene and 2.08 eV pentacene.

3.2.1. Pentacene. The results obtained by solving the BSE are considered to be the gold standard for the excitonic physics. Before testing the bootstrap xc kernel, it would be instructive to look at the accuracy of the BSE results; several BSE calculations have been done in the past for Pentacene crystal, and in Figure 5 we compare all these including the BSE results obtained in

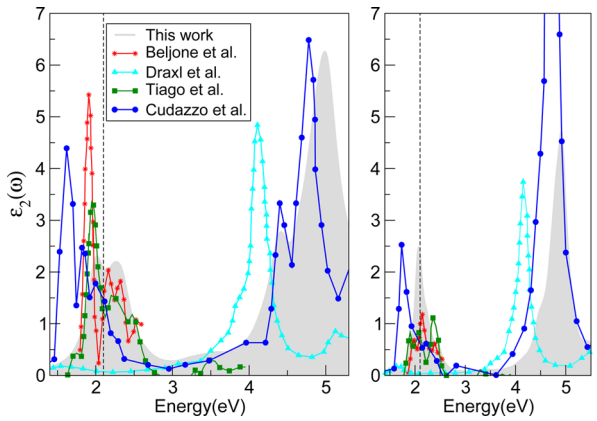

Figure 5. Dielectric tensor for pentacene, obtained by solving the BSE, as a function of energy (in electronvolts) in two different polarization directions (x and y). Previous BSE data is taken from refs 11, 12, and 20 and quantum chemical data is taken from ref 21. The quasi-particle gap is indicated by verticle dashed (black) line.

the present work. In Figure 5 are also presented the highly accurate quantum chemical data of Beljonne et al.[21] for comparison with these results obtained by solving the BSE. In the low-energy region (1−3 eV) optical spectra of Beljonne et al., Tiago et al.[20], and the present work are in good agreement with each other; all three show a single excitonic peak below the gap. The results of Cudazzo et al.[12] are slightly red-shifted (by ∼0.3 eV) with respect to all these works. The results of Ambrosch-Draxl et al.[11] are totally different in that there is almost no spectra weight in this energy window of 1−3 eV.

In the high-energy region (3.5−6 eV), the present results agree very well with the previous data of Cudazzo et al.[12]; however, the data of Ambrosch-Draxl et al.[11] are red-shifted. These differences perhaps could be attributed to computational parameters or the ground-state basis set used in various calculations. This spread of the BSE results point to limitations not of the BSE method itself but rather of the differences in various implementations. It is impossible to say from these results what the definitive BSE spectra should be for this material. The question we now ask ourselves is how close are the TDDFT results to their BSE counterpart? To answer this question, we determine the spectra using the bootstrap xc kernel within TDDFT, and the results are plotted in Figure 6.

We first look at the results obtained by including the LFE. Due to the low symmetry and molecular nature of the crystal, the dielectric function is highly anisotropic. There are no transitions up to an energy of 1.51 eV for light polarized along the x and y axes and 3.5 eV for the polarization axis along the z axis. The main peak in the dielectric functions occur at ∼5 eV for all three polarizations of light. In the low-energy region (1.5−3 eV), the response in the x direction shows a clear excitonic peak below the gap, indicating the presence of a bound exciton. In the y direction as well, there is substantial

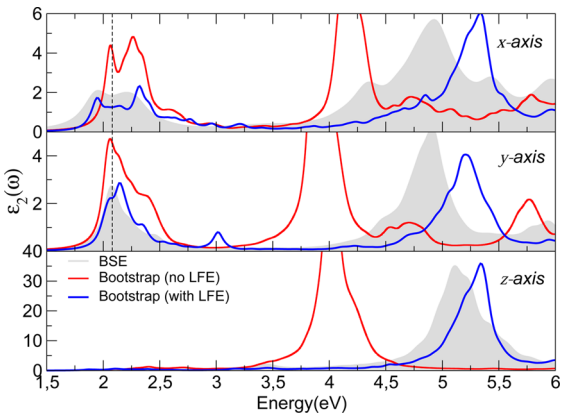

Figure 6. Dielectric tensor for pentacene obtained using the bootstrap kernel as a function of energy (in electronvolts) in three different polarization directions (x, y, and z). The quasi-particle gap is indicated by a dashed (black) line.

spectral weight below the gap. The difference in energy of the excitonic peak along the x and y axes is interpreted at the Davydov splitting.[12,18] TDDFT results give a value of Davydov splitting to be 0.18 eV, which is in agreement with the experimental data (0.15 eV).[22,23]

Now turning our attention to the differences between spectra with and without LFE, it is clear from Figure 6 that the TDDFT results in the low-energy region (<3 eV) obtained using the head only approximation (i.e., without LFE) are in agreement with the BSE results in terms peak positions but not in terms of the height of the peaks. On the other hand, in the high-energy range (>3 eV), results obtained without LFE are red-shifted with respect to the BSE results, and good agreement between TDDFT and BSE requires the inclusion of LFE within TDDFT. It is very interesting to note that TDDFT results with and without LFE, though substantially different from each other, lie in between the two extremes of various BSE data; in the high-energy region results obtained with LFE agree with BSE data of the present work and that of Cudazzo et al.,[12] while without LFE, the TDDFT results are in agreement with those of Ambrosch-Draxl et al.[11] In the low-energy range (1−3 eV), the TDDFT results obtained with LFE are in agreement with the BSE data of the present work and that of Tiago et al.[20]

3.2.2. Picene. The electron energy loss spectra (EELS) (i.e., the imaginary part of the inverse dielectric function) for solid picene is presented in Figure 7. The TDDFT spectra, calculated without LFE, in the xy plane (shown in the left panel) is in excellent agreement with the experimental data. We note that in terms of the relative peak heights and positions, the TDDFT results are in slightly better agreement with the experiments as compared to the BSE data (except for the initial peak at 3.3 eV, which is blue-shifted in the TDDFT results). For the polarization vector along the z axis, the TDDFT and the BSE results agree well with each other but not with the experimental data in the low-energy region (<5 eV). On the other hand, in the energy range above 5 eV, the agreement of the calculations (both TDDFT and BSE) with the experiments is much better. In the z direction, the TDDFT spectra with LFE is blue-shifted (in energy) with respect to the experimental data and is in better agreement with the BSE data of Roth et al.[40] We would also like to mention that picene shows no Davydov splitting in the absorption spectra (not shown here).

DOI: 10.1021/acs.jctc.5b00133
J. Chem. Theory Comput. XXXX, XXX, XXX−XXX

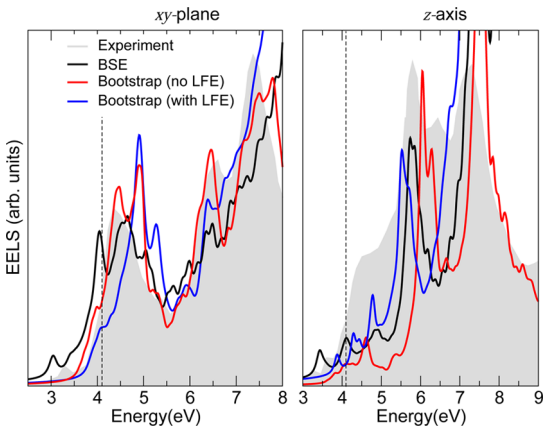

Figure 7. Electron energy loss spectra for picene obtained using the bootstrap kernel as a function of energy (in electron volts) in the *xy* plane (average of the response along the *x* and *y* axes) and along the *z* axis. The experimental and BSE data are taken from ref 40 indicated in the legend. The quasi-particle gap is indicated by a dashed (black) line.

4. CONCLUSIONS

To conclude, it is clear from these results that bootstrap method in its simplest and computationally most efficient form (i.e., using only the head of the xc kernel) consistently gives good results in the energy range most important for the design of solar cell materials (i.e., close to the band edge), thus constituting an excellent method for the study of the optical properties of organic materials. The strikingly different excitonic physics of picene and pentacene is very well captured by bootstrap; even subtle features such as the presence of a small Davydov splitting in pentacene and the absence of such in picene, are well-reproduced. We further note that for the case of pentacene, bootstrap results with and without local field effects, even though differ substantially from each other, are still not as different as BSE results obtained using different numerical implementations of the BSE. These results indicate that the head-only bootstrap kernel can be used to perform the first screening of 1000s of organic materials for designing solar cells followed by which more accurate calculations by solving BSE or by including LFE within TDDFT can be performed for selected prescreened interesting materials.

AUTHOR INFORMATION

Corresponding Author

*E-mail: sharma@mpi-halle.mpg.de.

Notes

The authors declare no competing financial interest.

REFERENCES

(1) Sham, L. J.; Rice, T. M. *Phys. Rev.* **1966**, *144*, 708−714.
(2) Hanke, W.; Sham, L. J. *Phys. Rev. Lett.* **1979**, *43*, 387−390.
(3) Runge, E.; Gross, E. K. U. *Phys. Rev. Lett.* **1984**, *52*, 997−1000.
(4) Reining, L.; Olevano, V.; Rubio, A.; Onida, G. *Phys. Rev. Lett.* **2002**, *88*, 066404.
(5) Sottile, F.; Olevano, V.; Reining, L. *Phys. Rev. Lett.* **2003**, *91*, 056402.
(6) Botti, S.; Fourreau, A.; Nguyen, F.; Renault, Y.-O.; Sottile, F.; Reining, L. *Phys. Rev. B* **2005**, *72*, 125203.
(7) Botti, S.; Schindlmayr, A.; Del-Sole, R.; Reining, L. *Rep. Prog. Phys.* **2007**, *70*, 357−407.
(8) Sharma, S.; Dewhurst, J. K.; Sanna, A.; Gross, E. K. U. *Phys. Rev. Lett.* **2011**, *107*, 186401.
(9) Sharma, S.; Dewhurst, J. K.; Sanna, A.; Rubio, A.; Gross, E. K. U. *New J. Phys.* **2012**, *14*, 053052.
(10) Ruini, A.; Caldas, M. J.; Bussi, G.; Molinari, E. *Phys. Rev. Lett.* **2002**, *88*, 206403.
(11) Ambrosch-Draxl, C.; Nabok, D.; Puschnig, P.; Meisenbichler, C. *New J. Phys.* **2009**, *11*, 125010.
(12) Cudazzo, P.; Gatti, M.; Rubio, A. *Phys. Rev. B* **2012**, *86*, 195307.
(13) Gross, E. K. U., Dobson, F. J., Petersilka, M. In *Topics in Current Chemisty. Density Functional Theory II*; Nalewajski, R. F., Ed.; Springer-Verlag: Heidelberg, 1996; Vol. *181*; pp 81−172.
(14) Mukamel, S.; Tretiak, S.; Wagersreiter, T.; Chernyak, V. *Science* **1997**, *277*, 781−787.
(15) Tian, B.; Zerbi, G.; Schenk, R.; Müllen, K. *J. Chem. Phys.* **1991**, *95*, 3191−3197.
(16) Halliday, D.; Burn, P.; Friend, R.; Bradley, D.; Holmes, A.; Kraft, A. *Synth. Met.* **1993**, *55*, 954−959.
(17) Alvarado, S. F.; Seidler, P. F.; Lidzey, D. G.; Bradley, D. D. C. *Phys. Rev. Lett.* **1998**, *81*, 1082−1085.
(18) Davydov, A. S. *Theory of Molecular Excitons*; McGraw-Hill: New York, 1962.
(19) Agranovich, V. M. *Excitations in Organic Solids*; Oxford University Press: Oxford, 2008.
(20) Tiago, M. L.; Northrup, J. E.; Louie, S. G. *Phys. Rev. B* **2003**, *67*, 115212.
(21) Beljonne, D.; Yamagata, H.; Brédas, J. L.; Spano, F. C.; Olivie, Y. *Phys. Rev. Lett.* **2013**, *110*, 226402.
(22) Dressel, M.; Gompf, B.; Faltermeier, D.; Tripathi, A. K.; Pflaum, J.; Schubert, M. *Opt. Express* **2008**, *16*, 19770−19778.
(23) Faltermeier, D.; Gompf, B.; Dressel, M.; Tripathi, A. K.; Pflaum, J. *Phys. Rev. B* **2006**, *74*, 125416.
(24) Rohlfing, M.; Louie, S. G. *Phys. Rev. Lett.* **1999**, *82*, 1959−1962.
(25) Botti, S.; Vast, N.; Reining, L.; Olevano, V.; Andreani, L. *Phys. Rev. B* **2004**, *70*, 045301.
(26) Singh, D. J. *Planewaves Pseudopotentials and the LAPW Method*; Kluwer Academic Publishers: Boston, 1994.
(27) The Elk FP-LAPW Code. http://elk.sourceforge.net (accessed March 12, 2015).
(28) Tran, F.; Blaha, P. *Phys. Rev. Lett.* **2009**, *102*, 226401.
(29) Singh, D. J. *Phys. Rev. B* **2010**, *82*, 205102.
(30) Lopata, K.; Reslan, R.; Kowalska, M.; Neuhauser, D.; Govind, N.; Kowalski, K. *J. Chem. Theory Comput.* **2011**, *7*, 3686−3693.
(31) Marian, C. M.; Gilka, N. *J. Chem. Theory Comput.* **2008**, *4*, 1501−1515.
(32) Wong, B. M.; Hsieh, T. H. *J. Chem. Theory Comput.* **2010**, *6*, 3704−3712.
(33) Grimme, S.; Parac, M. *Chem. Phys. Chem.* **2003**, *3*, 292−295.
(34) Richard, R.; Herbert, J. M. *J. Chem. Theory Comput.* **2011**, *7*, 1296−1306.
(35) Goerigk, L.; Grimme, S. *J. Am. Theory Comput.* **2011**, *7*, 3272−3277.
(36) Zimmerman, P. M.; Bell, F.; Casanova, D.; Head-Gordon, M. *J. Am. Chem. Soc.* **2011**, *133*, 19944−19952.
(37) Campbell, R. B.; Robertson, J. M.; Trotter, J. *Acta Crystallogr.* **1962**, *15*, 289−290.
(38) Mattheus, C. C.; Dros, A. B.; Baas, J.; Meetsma, A.; de. Boer, J. L.; Palstra, T. T. M. *Acta Crystallogr., Sect. C* **2001**, *57*, 939−941.
(39) Ghosh, A. D. R.; Roychowdhury, S.; Roychowdhury, P. *Acta Crystallogr., Sect. C* **1985**, *41*, 907−909.
(40) Roth, F.; Gatti, M.; Cudazzo, P.; Grobosch, M.; Mahns, B.; Büchner, B.; Rubio, A.; Knupfer, M. *New J. Phys.* **2010**, *12*, 103036.

DOI: 10.1021/acs.jctc.5b00133
J. Chem. Theory Comput. XXXX, XXX, XXX−XXX